

The discrimination of mass hierarchy with atmospheric neutrinos at a magnetized muon detector

Abhijit Samanta *

Harish-Chandra Research Institute, Chhatnag Road, Jhusi, Allahabad 211 019, India

(Dated: October 30, 2018)

We have studied the mass hierarchy with atmospheric neutrinos considering the muon energy and zenith angle of the event at the magnetized iron calorimeter detector. For χ^2 analysis we have migrated the number of events from neutrino energy and zenith angle bins to muon energy and zenith angle bins using the two-dimensional energy-angle correlated resolution functions. The binning of data is made in two-dimensional grids of $\log_{10} E - L^{0.4}$ plane to get a better reflection of the oscillation pattern in the χ^2 analysis. Then the χ^2 is marginalized considering all possible systematic uncertainties of the atmospheric neutrino flux and cross section. The effects of the ranges of oscillation parameters on the marginalization are also studied. The lower limit of the range of θ_{13} for marginalization is found to be very crucial in determining the sensitivity of hierarchy for a given θ_{13} . Finally, we show that one can discriminate atmospheric neutrino mass hierarchy at $>90\%$ C.L. if the lower limit of $\theta_{13} \geq 5^\circ$.

PACS numbers: 14.60.Pq

I. INTRODUCTION

The origin of masses of the particles and their interactions have been successfully described by the standard model (SM). The recent discovery of neutrino masses and their mixing through neutrino oscillation [1, 2] opens a new window beyond the SM. This provides the measurements of mass squared differences $\Delta m_{ji}^2 = m_j^2 - m_i^2$ and mixing angles θ_{ij} . At present $1(3)\sigma$ ranges are [3]: $\Delta m_{21}^2 = 7.67_{-0.19}^{+0.16}({}_{-0.53}^{+0.42}) \times 10^{-5} \text{eV}^2$, $|\Delta m_{31}^2| = 2.39_{-0.018}^{+0.11}({}_{-0.049}^{+0.063}) \times 10^{-3} \text{eV}^2$, $\sin^2 \theta_{12} = 0.312_{-0.018}^{+0.019}({}_{-0.049}^{+0.063})$, $\sin^2 \theta_{23} = 0.466_{-0.073}^{+0.058}({}_{-0.135}^{+0.178})$, and $\sin^2 \theta_{13} = 0.016_{-0.010}^{+0.010} (< 0.046)$. Here θ_{ij} are the mixing angles in Pontecorvo, Maki, Nakagawa, Sakata mixing matrix [4]. Currently, there is no constraint on the CP violating phase δ_{CP} or on the sign of Δm_{31}^2 . The neutrino mass ordering is one of the key problems to build up the fundamental theory of the particles beyond the SM. This can be probed through neutrino oscillation. In this paper we have concentrated on the prospects to resolve the mass hierarchy using atmospheric neutrinos.

The mass hierarchy with atmospheric neutrinos has been studied in [5–7] with a large magnetized Iron CALorimeter (ICAL) detector, which is being strong considered for the India-based Neutrino Observatory [8]. In [9], the authors estimated the sensitivity of a large liquid argon detector. This is nonmagnetized, but can detect both electron and muon. So, here the statistics are high compared to ICAL. However, these studies have

dealt with neutrino energy and zenith angle and assumed fixed Gaussian resolutions for them separately. It is also shown that the confidence level of determining hierarchy changes drastically with the change in width of resolutions. Moreover, since all of the particles produced in the neutrino interactions can not be reconstructed, the resolutions are not Gaussian in nature. There are many neutral particles in the deep inelastic processes, and the non-Gaussian nature of the resolutions increases as one goes to higher energies. Again, the resolutions are different for neutrino and antineutrino (see Fig. 4 of [10]) since the different quantum numbers are involved in the scattering matrix elements for neutrino and antineutrino. At energies around 1 GeV, most of the events are quasi-elastic, and the muon carries almost all of the energy of the neutrino. Here, the energy resolution is very good. As the energy increases, the deep inelastic process dominates and the energy resolution begins to worsen by developing a more prominent non-Gaussian nature. However, the trend of angular resolution is quite opposite, its width is very wide at low energy, and it improves with an increase in energy. So, it is very important to study the sensitivity of a detector in terms of directly measurable quantities.

We have studied the neutrino mass hierarchy for the magnetized ICAL detector with atmospheric neutrinos generating events by NUANCE-v3 [11] and considering the muon energy and direction (directly measurable quantities) of the event. Because of heavy mass of the muon, it loses energy mostly via ionization and atomic excitation during its propagation through a medium. Since ICAL is a tracking detector, it gives a clean single track in the detector. The muon energy can be measured from the bending of the track in the magnetic field

*E-mail address: abhijit@hri.res.in

or from the track length in the case of a fully contained event. The direction can be measured from the tangent of the track at the vertex. From the GEANT [12] simulation of the ICAL detector it is found that the energy and angular resolutions of the muons are very high (4-10% for energy and 4-12% for zenith angle) and negligible compared to the resolutions obtained from the kinematics of the scattering processes. A new method for migration from true neutrino energy and zenith angle to muon energy and zenith angle has been introduced in [13] and subsequently used in [10, 14, 15].

On the other hand, the binning of the data is also an important issue when one considers the binning of the events in reconstructed energy and zenith angle bins. The reasons are the following: The atmospheric neutrino flux changes very rapidly with energy following a power law (roughly $\sim E^{-2.8}$). Again, the behavior of the oscillation probability changes with the change in zones of $E - L$ plane. This has been discussed in [10, 14]. In case of proper binning of the data [10], the precision of oscillation parameters improves. Then it helps in hierarchy discrimination by reducing the effect of the ranges of the parameters, over which the marginalization is carried out.

In our previous work [13], the χ^2 analysis has been carried out considering the ratio of total up and total down going events for each resonance zone. Since the ratio up/down cancels all overall uncertainties, we considered only the energy dependent one. However, it should be noted here that the ratio of two Gaussian observables is not an exact Gaussian function. Our previous χ^2 study assuming the up/down ratio as a Gaussian function was motivated by the cancellations of all overall uncertainties. So, the result was an approximated one.

It is important to estimate the sensitivity of hierarchy determination with realistically measurable parameters of the experiments through a detailed analysis. Here, we have performed the χ^2 analysis following Poissonian distribution and considering the number of events in the grids of the $\log_{10} E - L^{0.4}$ plane of the muon. This follows Poissonian (Gaussian) distribution for a less (large) number of events. For a large number of events Poissonian distribution tends to a Gaussian one. We have taken into account all possible systematic uncertainties using the pull method of the χ^2 analysis. Expecting the lower bound of θ_{13} to be known from other experiments like Double Chooz [16] or NO ν A [17], we have also estimated the improved sensitivity considering the lower bound of θ_{13} for marginalization as the input value of θ_{13} for generating the experimental data for the χ^2 analysis.

II. OSCILLATION FORMALISM

To understand the analytical solution of time evolution of neutrino propagation through matter, we adopt the so-called ‘‘one mass scale dominance’’ framework: $|\Delta m_{21}^2| \ll |m_3^2 - m_{2,1}^2|$ [18, 19].

With this one mass scale dominance approximation, the survival probability of ν_μ can be expressed as

$$P_{\mu\mu}^m = 1 - \cos^2 \theta_{13}^m \sin^2 2\theta_{23} \\ \times \sin^2 \left[1.27 \left(\frac{(\Delta m_{31}^2) + A + (\Delta m_{31}^2)^m}{2} \right) \frac{L}{E} \right] \\ - \sin^2 \theta_{13}^m \sin^2 2\theta_{23} \\ \times \sin^2 \left[1.27 \left(\frac{(\Delta m_{31}^2) + A - (\Delta m_{31}^2)^m}{2} \right) \frac{L}{E} \right] \\ - \sin^4 \theta_{23} \sin^2 2\theta_{13}^m \sin^2 \left[1.27 (\Delta m_{31}^2)^m \frac{L}{E} \right] \quad (1)$$

The mass squared difference $(\Delta m_{31}^2)^m$ and mixing angle $\sin^2 2\theta_{13}^m$ in matter are related to their vacuum values by

$$(\Delta m_{31}^2)^m = \sqrt{((\Delta m_{31}^2) \cos 2\theta_{13} - A)^2 + ((\Delta m_{31}^2) \sin 2\theta_{13})^2} \\ \sin 2\theta_{13}^m = \frac{(\Delta m_{31}^2) \sin 2\theta_{13}}{\sqrt{((\Delta m_{31}^2) \cos 2\theta_{13} - A)^2 + ((\Delta m_{31}^2) \sin 2\theta_{13})^2}} \quad (2)$$

where, the matter term $A = 2\sqrt{2}G_F n_e E = 7.63 \times 10^{-5} \text{ eV}^2 \rho(\text{gm/cc}) E(\text{GeV}) \text{ eV}^2$. Here, G_F and n_e are the Fermi constant and the electron number density in matter and ρ is the matter density. The evolution equation for antineutrinos has the sign of A reversed.

From Eqs. 1 and 2 it is seen that a resonance in $P_{\mu\mu}^m$ will occur for neutrinos (antineutrinos) with normal hierarchy (inverted hierarchy) when

$$\sin^2 2\theta_{13}^m \rightarrow 1 \quad \text{or,} \quad A = \Delta m_{31}^2 \cos 2\theta_{13}. \quad (3)$$

Then resonance energy can be expressed as

$$E = \left[\frac{1}{2 \times 0.76 \times 10^{-4} Y_e} \right] \left[\frac{|\Delta m_{31}^2|}{\text{eV}^2} \cos 2\theta_{13} \right] \left[\frac{\text{gm/cc}}{\rho} \right] \quad (4)$$

The difference ΔP between $P_{\mu\mu}(\Delta m_{31}^2)$ and $P_{\mu\mu}(-\Delta m_{31}^2)$ has been plotted in Fig. 1 for ν_μ and $\bar{\nu}_\mu$ with $\theta_{13} = 2^\circ$ and $\theta_{13} = 10^\circ$, respectively, as an oscillogram in a two-dimensional plane of $E - \cos \theta^{\text{nadir}}$. We see that there exists a difference in all $E - \cos \theta^{\text{nadir}}$ space. This is not due to the matter effect, but due to the nonzero value of Δm_{21}^2 . So this exists for $\theta_{13} = 0^\circ$ also. It is seen that the resonance zones are different for ν and $\bar{\nu}$ and both their areas and amplitudes squeeze with a decrease in θ_{13} values.

III. THE χ^2 ANALYSIS

The χ^2 is calculated according to the Poisson probability distribution. The binning the data is made in two-dimensional grids in the plane of $\log_{10} E - L^{0.4}$ of the muon. The method for migration of number of events from neutrino to muon energy and zenith angle bins, the number of bins, the systematic uncertainties, and the cuts at the near horizons are described in [14].

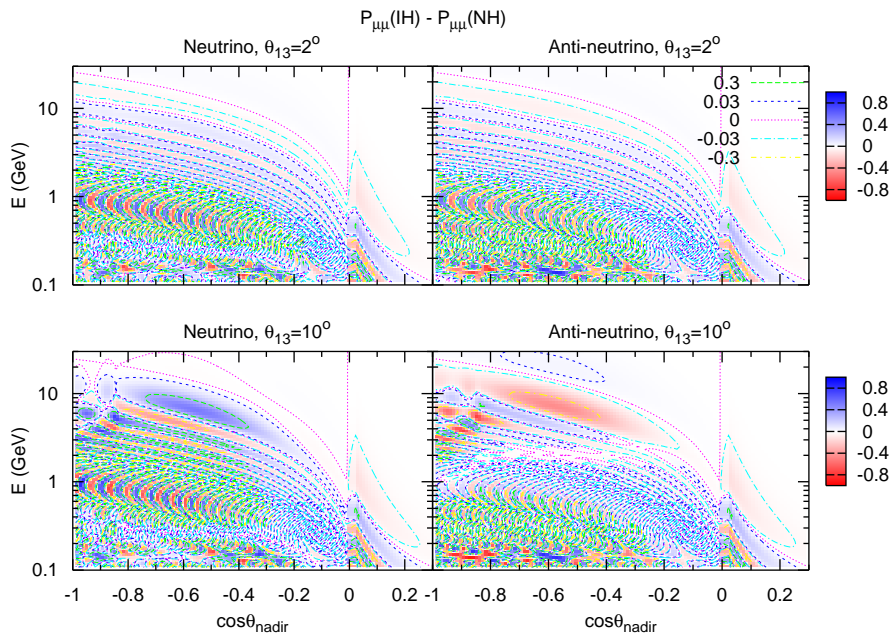


FIG. 1: The oscillogram of the difference $P_{\mu\mu}(-\Delta m_{31}^2) - P_{\mu\mu}(\Delta m_{31}^2)$ in the $E - \cos\theta_{\text{nadir}}$ plane for $\theta_{13} = 2^\circ$ (top) and $\theta_{13} = 10^\circ$ (bottom) with ν_μ (left) and $\bar{\nu}_\mu$ (right), respectively. We set $|\Delta m_{32}^2| = 2.5 \times 10^{-3} \text{eV}^2$, $\theta_{23} = 45^\circ$, $\delta_{CP} = 180^\circ$, and other oscillation parameters at their best-fit values.

The fact is that neutrino cross sections have not been precisely measured at all energies, and the neutrino flux is also not precisely known at every energy. There may arise an energy dependent systematic uncertainty. We may not always realize this. The program NUANCE considers difference processes of interactions at different energies using the Monte Carlo method. This may not be fully captured when we generate theoretical data by folding the flux with total cross section and smearing with the resolution functions[10]. The similar situation may happen in real experiments also. The mass hierarchy is determined considering the difference in number of events between normal hierarchy (NH) and inverted hierarchy (IH). This arises for the resonance in neutrino propagation through matter. It happens for some particular zones of energy and the baseline. So, there may arise a large difference in estimated hierarchy sensitivities with and without consideration of this systematic uncertainty. One can generate the experimental data for χ^2 analysis in two ways: I) directly from NUANCE simulation for a given set of oscillation parameters with 1 Mton.year exposure and then binning the events in muon energy and zenith angle bins; II) considering the oscillated atmospheric neutrino flux for a given set of parameters and then folding with time of exposure, total cross section, detector mass and finally smearing it with the energy-angle correlated resolution functions. This is similar with the method of generating the theoretical data for χ^2 analysis.

One can generate the theoretical data directly from a huge data set, say, 500 Mton.year data (to ensure the

statistical error negligible) for **each** set of oscillation parameters and then reducing it to 1 Mton.year equivalent data from it, which would be the more straightforward way for method I of generating experimental data. In this case, the effect of the above systematic uncertainty will not come into the play. The marginalization study with this method is almost an undoable job in a normal CPU. When we adopt different methods for generating theoretical and experimental data, the significant effect of the above systematic uncertainties come into the results. So, we adopt the same method for them and here we consider method II.

IV. RESULTS

We marginalize the χ^2 over all the oscillation parameters Δm_{32}^2 , θ_{23} , θ_{13} , and δ_{CP} along with solar oscillation parameters Δm_{21}^2 and θ_{12} for both NH and IH with ν_s and $\bar{\nu}_s$ separately for a given set of input data. Then we find the total $\chi^2 [= \chi_\nu^2 + \chi_{\bar{\nu}}^2]$.

We have chosen the range of $\Delta m_{32}^2 = 2.0 - 3.0 \times 10^{-3} \text{eV}^2$, $\theta_{23} = 37^\circ - 54^\circ$, $\theta_{13} = 0^\circ - 12.5^\circ$ and $\delta_{CP} = 0^\circ - 360^\circ$. We set the range of $\Delta m_{21}^2 = 7.06 - 8.34 \times 10^{-5} \text{eV}^2$ and $\theta_{12} = 30.5^\circ - 40^\circ$. However, the effect of Δm_{21}^2 comes in the subleading order in the oscillation probability when $E \sim \text{GeV}$ and it is marginal. We set the input of atmospheric oscillation parameters $|\Delta m_{32}^2| = 2.5 \times 10^{-3} \text{eV}^2$, $\theta_{23} = 45^\circ$, and $\delta_{CP} = 180^\circ$ and the solar parameters $\Delta m_{21}^2 = 7.9 \times 10^{-5} \text{eV}^2$ and $\theta_{12} = 33^\circ$. We set IH as in-

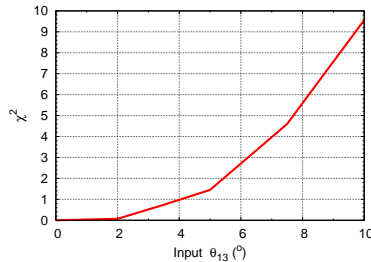


FIG. 2: The variation of marginalized χ^2 (false) with different input values of θ_{13} .

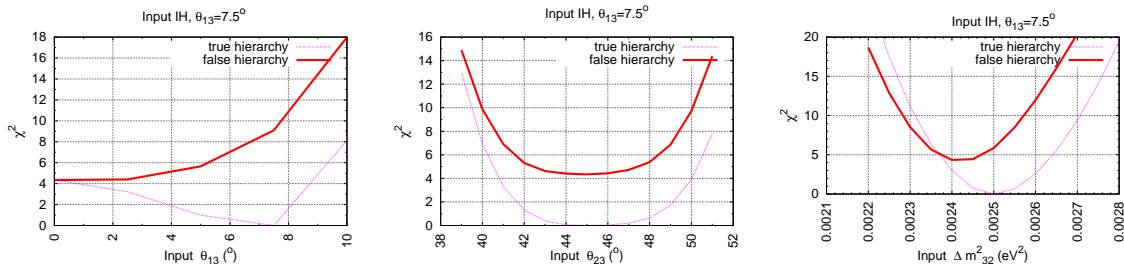


FIG. 3: The variation of χ^2 with θ_{13} , θ_{23} , and Δm_{32}^2 , respectively for both true and false hierarchy. The χ^2 is marginalized with respect to all oscillation parameters except with which it varies.

put. The variation of marginalized χ^2 for different input values of θ_{13} is shown in Fig. 2.

To see the effect of marginalization over the ranges of parameters, we have shown the variation of χ^2 for both true and false hierarchy as a function of θ_{13} , θ_{23} and $|\Delta m_{32}^2|$ in Fig. 3. Here, we have marginalized the χ^2 over all oscillation parameters except one with which it varies. We find that significant improvement will come if the lower bound of θ_{13} improves from zero. This is demonstrated in the first plot in Fig. 3. We also see from this figure that there is no significant effect of other parameters on marginalization since they are well determined in this experiment. We find from Fig. 4 that if the lower limit is 5° , the mass hierarchy can be determined at a confidence level $> 90\%$.

The absolute bounds of each oscillation parameter can also be seen in Fig. 3 when one sees the curve for its true hierarchy. It should be noted here that in the case of method II, the best-fit values are same with their input

values, which is not always the case in analysis using method I (discussed in [10]). However, the precision of the parameters is almost same here with method I (which is used in our previous work [10]).

We have further studied for the cases when the lower limit of the range of θ_{13} for marginalization is the input value for the experimental data set. Considering this constraint we have plotted the variation of χ^2 with input values of θ_{13} in Fig. 5. This will give the lower limit of the sensitivity of the mass hierarchy in this detector when the lower limit of θ_{13} is known from other experiments like Double Chooz [16] or NO ν A [17]. A significant improvement is observed comparing Figs. 2 and 5.

Acknowledgments: This research has been supported by funds from Neutrino Physics projects at HRI. The use of excellent cluster computational facility installed by the funds of this project is also gratefully acknowledged. The general cluster facility of HRI has also been used at the initial stages of the work.

-
- [1] B. Pontecorvo, J. Exp. Theor. Phys. **33**, 549 (1957); Sov. Phys. JETP, **6**, 429 (1958).
[2] Y. Fukuda *et al.* [Super-Kamiokande Collaboration], Phys. Rev. Lett. **81**, 1562 (1998) [arXiv:hep-ex/9807003].
[3] G. L. Fogli *et al.*, Phys. Rev. D **78**, 033010 (2008) [arXiv:0805.2517 [hep-ph]].
[4] Z. Maki, M. Nakagawa and S. Sakata, Prog. Theor. Phys. **28**, 870 (1962). B. Pontecorvo, JETP **6** (1958) 429; **7** (1958) 172;
[5] D. Indumathi and M. V. N. Murthy, Phys. Rev. D **71**, 013001 (2005) [arXiv:hep-ph/0407336].
[6] R. Gandhi, P. Ghoshal, S. Goswami, P. Mehta, S. U. Sankar and S. Shalgar, Phys. Rev. D **76**, 073012 (2007) [arXiv:0707.1723 [hep-ph]].
[7] S. T. Petcov and T. Schwetz, Nucl. Phys. B **740**, 1 (2006) [arXiv:hep-ph/0511277].
[8] See “India-based Neutrino Observatory: Project Report. Volume I,” available at <http://www.imsc.res.in/~ino/>
[9] R. Gandhi, P. Ghoshal, S. Goswami and S. Uma Sankar, Phys. Rev. D **78**, 073001 (2008) [arXiv:0807.2759 [hep-ph]].

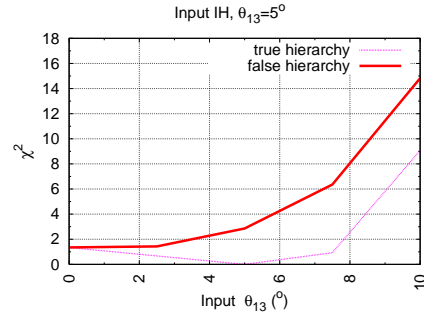


FIG. 4: The same as Fig. 3, but with θ_{13} only and with input $\theta_{13} = 5^\circ$.

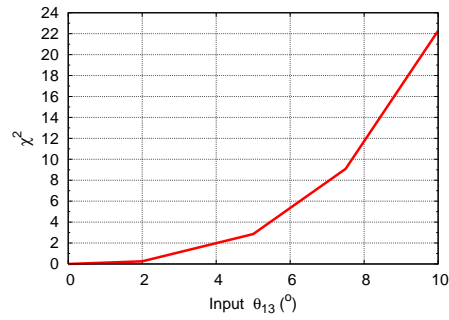


FIG. 5: The same as Fig. 2, but the lower limit of the range of θ_{13} for marginalization is the corresponding input value used for generating the experimental data set. This gives the lower limit of the sensitivity corresponding to a lower limit of θ_{13} obtained from other experiments.

- ph]].
- [10] A. Samanta, Phys. Rev. D **80**, 113003 (2009) [arXiv:0812.4639 [hep-ph]].
- [11] D. Casper, Nucl. Phys. Proc. Suppl. **112**, 161 (2002) [arXiv:hep-ph/0208030].
- [12] <http://geant4.web.cern.ch/geant4/>
- [13] A. Samanta, Phys. Lett. B **673**, 37 (2009) [arXiv:hep-ph/0610196].
- [14] A. Samanta, Phys. Rev. D **79**, 053011 (2009) [arXiv:0812.4640 [hep-ph]].
- [15] A. Samanta, Phys. Rev. D **80**, 073008 (2009) [arXiv:0907.3978 [hep-ph]].
- [16] F. Ardellier *et al.* [Double Chooz Collaboration], arXiv:hep-ex/0606025.
- [17] D. S. Ayres *et al.* [NOvA Collaboration], arXiv:hep-ex/0503053.
- [18] O. L. G. Peres and A. Y. Smirnov, Nucl. Phys. B **680** (2004) 479 [arXiv:hep-ph/0309312].
- [19] E. K. Akhmedov, R. Johansson, M. Lindner, T. Ohlsson and T. Schwetz, JHEP **0404** (2004) 078 [arXiv:hep-ph/0402175].